JOURNAL OF Applied Polymer SCIENCE

In Situ Biaxial Stretching for the Platelet Formation of an Ethylene–Vinyl Alcohol Copolymer Through Multistage Stretching Extrusion and Its Effect on the Gas-Barrier Properties of Polyethylene

Jiaming Zhu, Jiabin Shen, Shaoyun Guo

State Key Laboratory of Polymer Materials Engineering, Polymer Research Institute, Sichuan University, Chengdu Sichuan 610065, People's Republic of China

Correspondence to: J. Shen (E-mail: shenjb@scu.edu.cn) or S. Guo (E-mail: nic7702@scu.edu.cn)

ABSTRACT: The morphological evolution of ethylene–vinyl alcohol copolymer (EVOH) and its effect on the gas-barrier properties of high-density polyethylene (HDPE) were investigated. HDPE/EVOH blends were prepared through a multistage stretching extrusion, which combined an assembly of force-assembling elements (FAEs) with an extruder. Scanning electron microscopy confirmed that with an increasing number of FAEs, the biaxial-stretching field existing in each FAE transformed the dispersed EVOH phase into well-defined platelets along the flowing plane. Dynamic rheological results further revealed that the formation of the platelets enlarged the interfaces between the dispersed barrier phase and the matrix; this not only led to the decline of the complex viscosity but also created more tortuous paths for the diffusion of gas molecules. Compared with that of the non-FAE specimen blended with 25 wt % EVOH, the oxygen permeability coefficient decreased more than one order of magnitude when one FAE was applied. The structural model for permeability indicated that the enhanced barrier resulted from the increased tortuosity of the diffusion pathway, which was provided by the aligned high-aspect-ratio platelets. Compared with the previous biaxial-stretching method, multistage stretching extrusion provided a simple and economical way to generate a laminar structure of the dispersed phase in the matrix phase without the application of an external stretching force. © 2013 Wiley Periodicals, Inc. J. Appl. Polym. Sci. **2014**, *131*, 40221.

KEYWORDS: blends; extrusion; structure; property relations

Received 8 July 2013; accepted 21 November 2013

DOI: 10.1002/app.40221

INTRODUCTION

For its lightness, flexibility, transparency, and ease of processing, high-density polyethylene (HDPE) has attached much attention in the packaging field. However, its high permeability to oxygen brings it unexpected limitations.[1,2] Although ethylene–vinyl alcohol copolymer (EVOH) is known to be an ideal substitute, its sensitive permeation resistance to humid conditions and its high price need to be considered. Thus, the blending of EVOH with HDPE turns out to be an advisable method for the preparation of low-cost and highly effective gas-barrier products.[3–5]

In past decades, multilayer coextrusion has been verified as an effective way to fabricate gas-barrier materials with a multilayered structure.[6–8] For example, Lei et al.[9] prepared oxygen barrier films consisting of alternating layers of HDPE and polyamide 6. The results show that the permeability coefficient decreased about one order of magnitude and became much closer to that of pure polyamide 6 as the number of layers was increased from 2 to 128. Hiltner and coworkers[10–12] also prepared a series of alternating multilayered materials with thousands of layers. It was found that the nanoscale thickness of each layer induced the confined crystallization of polymeric materials. The highly ordered intralayer lamellae structure further increased the tortuous pathways of the gas molecules and led to a distinct decrease in the permeability coefficient. Although the multilayered structure is regarded as the best choice for limiting gas diffusion, the poor compatibility and the viscosity mismatch between adjacent layers may cause a weak interfacial adhesion and an unstable structure.[13–15] Hence, the barrier phase dispersed like platelets in the matrix is still widely applied to provide a low permeability for an immiscible system.[16–18]

Many researchers have contributed a lot to the fabrication of permeability barriers by controlling the morphology of polymer blends.[19–24] As a matter of fact, in most polymer blending processes, the phase morphology is an outcome of the interplay of breakup and coalescence.[25–27] To obtain a plateletlike morphology, intermediate compositions are sometimes necessary such that large bodies arising from significant coalescence during compounding can be readily extended. However, an increase in

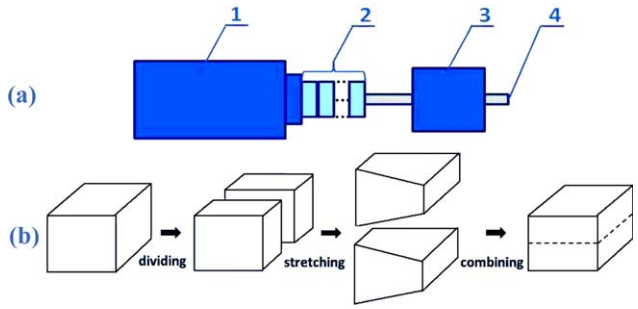

Figure 1. Schematic of (a) the multistage stretching extrusion system [(1) single-screw extruder, (2) assembly of FAEs, (3) water-cooling block, and (4) sample] and (b) the flowing behavior of a melt in an FAE. [Color figure can be viewed in the online issue, which is available at wileyonlinelibrary.com.]

the cost and the deterioration of certain ancillary properties may become inevitable.[28] Hence, the attainment of an expected morphology at a low composition deserves more attentions.

In the common case, the phase with a low composition may be dispersed like droplets. To extend them into a plateletlike morphology, a corresponding force field is necessary. For example, Yeo et al.[29] reported that as the as-cast polypropylene (PP)/EVOH blend experienced a biaxial stretching, a well-developed laminar structure of the dispersed phase was generated; this led the oxygen permeability [$P_{(O2)}$] to decrease about 10 times relative to that of the pure PP. This leads to the thought that if the biaxial stretching can be introduced into the compounding process, the plateletlike morphology may be attained *in situ* without postprocessing. Kwon and Zumbrunnen[30] used a chaotic mixing method to fabricate an LDPE/EVOH blend with well-developed platelets. The large component bodies were stretched and folded by the application of both batch and continuous flow devices. The method offers an idea that folding or multiplying would be useful for the deformation of the dispersed phase.

Recently, a biaxial–multistage stretching extrusion technology was developed on the basis of force-assembling coextrusion technology.[31–33] In contrast to the coextrusion system, an assembly of force-assembling elements (FAEs) is combined with only one extruder [Figure 1(a)]. The flowing behavior of a blended melt in a FAE is divided into three stages [Figure 1(b)]: dividing, biaxial stretching, and combining. When the melt enters an FAE, it is first evenly sliced by a divider into left and right parts, and then, each of them flows into a fishtail duct. It has been revealed that the flowing behavior in the fishtail duct can be regarded as the combination of extending flow and convergent flow; this may provide a biaxial-stretching field for the melt.[34] At the exit of the FAE, a combining process takes place to combine the two stretched parts together. If the melt flows into the next FAE, the dividing–stretching–multiplying process may be repeated. Hence, it can be imagined that the morphology of the dispersed phase may be controlled by the number of FAEs.

In this study, HDPE/EVOH blends with different compositions were extruded by the application of different numbers of FAEs. The morphological evolution of the EVOH phase was verified by scanning electronic microscopy (SEM), and its effects on the dynamic rheological behaviors and the gas-barrier properties were investigated.

EXPERIMENTAL

Materials

The polymers used in this study were HDPE (6098) and EVOH (DC3212). The HDPE, with a density of 0.951 g/cm^3, was produced by Qi Lu Petroleum Chemical Co., Ltd. (China). The EVOH, consisting of 32 mol % ethylene and with a density of 1.19 g/cm^3, was obtained from Nippon Synthetic Chemical Industry Co., Ltd. (Japan).

Specimen Preparation

HDPE and EVOH were dried in a vacuum oven at 85°C for 12 h. These raw materials were physically mixed together in a high-speed mixer at room temperature before extrusion and were then melt-blended into the HDPE/EVOH pellets by extrusion through a twin-screw extruder. Subsequently, these dried pellets were extruded from the multistage stretching extrusion system, as illustrated in Figure 1(a). The melt flowed through an extruder, an assembly of FAEs, and a water-cooling block and then formed a film about 1.0 mm thick and 40 mm wide. The temperature from the die of the extruder to the FAEs was maintained at 200°C, and the temperature of the water-cooling block was room temperature, around 23°C.

Capillary Rheometer

A high-pressure capillary rheometer (Rosand RH7, Bohlin Instruments, United Kingdom) was used to measure the shear viscosities of the pure EVOH and HDPE at 200, 210, and 220°C with a capillary die with a 1-mm diameter and a length/diameter ratio of 30. The measurements were corrected by the Rabinowitsch and Bagley equations. The viscosities of the pure HDPE and EVOH and their viscosity ratios measured at 153.4, 259.2, and 431.7 s^{-1} are listed in Table I. The results show that at the same shear rate, the viscosity of EVOH was lower than that of HDPE, whereas the former got closer to the latter with

Table I. Shear Viscosity for the Pure HDPE and EVOH and Their Viscosity Ratios

		Shear viscosity (Pa s)		
	Shear rate (s^{-1})	HDPE	EVOH	HDPE/EVOH viscosity ratio
200°C	153.4	1545.5	428.5	3.6
	259.2	1106.0	377.1	2.9
	431.7	563.9	330.8	1.7
210°C	153.4	1425.1	370.8	3.8
	259.2	1008.5	329.6	3.1
	431.7	690.8	285.8	2.4
220°C	153.4	1295.7	303.6	4.3
	259.2	902.6	279.7	3.2
	431.7	641.4	251.1	2.6

decreasing temperature. It is well understood[27] that at a same composition, a closer viscosity tends to form a larger size of dispersed phase, which might be more easily deformed in the external force field. Hence, in this study, the HDPE/EVOH blends were extruded at 200°C to obtain a closer viscosity between HDPE and EVOH.

SEM

A scanning electron microscope (JSM-5900LV, Japan) was used to examine the morphology of the dispersed EVOH phase. Each specimen was quenched in liquid nitrogen for 3 h and cryofractured vertically to the machine direction. The fractured surface was coated with a layer of gold in a vacuum chamber for conductivity.

Dynamic Rheological Analysis

Dynamic rheological measurements were performed on a dynamic oscillatory rheometer (AR1500ex, TA Instrument). Each measurement was run with a 25-mm diameter parallel-plate geometry and a 1.0-mm sample gap. The dynamic viscoelastic properties were determined with frequencies from 0.01 to 100 Hz with a 2% strain value determined with a stress sweep to keep it within the linear viscoelastic region. Measurements were carried out at 170°C under a nitrogen atmosphere so that the EVOH phase remained its solid state.

Gas Permeability Test

The gas permeability test was performed with a pressure differential gas permeation instrument (VAC-V1) produced by Labthink Instrument Co. (China). The instrument included an upper chamber, where the gas pressure was maintained at 0.5 MPa, and a lower chamber, which was vacuumed for 12 h before testing. The specimen, with a diameter of 50 mm and a thickness of 1 mm, was placed between the upper and lower chambers. The test temperature was maintained at 40°C and 12.5% relative humidity to maintain stable operation of the equipment, according to the suggestion of the manufacturer. In this study, the oxygen and carbon dioxide permeability [$P_{(CO2)}$] coefficients were measured under the same conditions.

RESULTS AND DISCUSSION

The morphological evolution of the HDPE/EVOH blend after the multistage stretching extrusion was examined by SEM. The cross-sectional morphologies (vertical to the machine direction) of the system filled with 25 wt % EVOH and prepared by the application of different numbers of FAEs are compared in Figure 2(a–d). For the non-FAE specimen [Figure 2(a)], the cross sections of most of the EVOH phase were elliptical in shape; this indicated that there was weak deformation vertical to the machine direction. When one FAE was applied [Figure 2(b)], some of the elliptical particles became thinner and were extended along the transverse direction. With a further increase in the number of FAEs to two or even three [Figure 2(c,d)], the SEM images of the cross sections of the specimens revealed much more well-defined platelets dispersed in the matrix and aligned in parallel. As described previously, when the melt entered an FAE, it flowed through a fishtail duct, which became wider and thinner from the entrance to the exit. The flowing behavior of the melt could be regarded as a combination of extending flow and convergent flow; this caused the *in situ* expansion of the dispersed phase in the flowing plane, as schematically illustrated in Figure 2(e). Hence, the application of more FAEs, which could provide an iterative biaxial-stretching field, might have further promoted the expansion of the plateletlike morphology in the melt-extrusion process and led to an extremely tortuous path for the diffusing gas molecules. In contrast, the conventional biaxial-stretching method[29,35,36] is generally applied after the casting and cooling of films; this might induce better molecular orientation and higher crystallization so that the permeability of gas molecules can be reduced.

The expansion of the EVOH phase accompanying the increase in the number of FAEs was further detected by dynamic rheological testing at 170°C, which was intermediate between the melting temperatures of HDPE and EVOH, so that the dispersed phase remained its initial morphology. The dependence of the complex viscosity of the specimens blended with 15, 20, 25, and 35 wt % EVOH on the frequency is shown in Figure 3. We found that all of the specimens were typical pseudoplastic materials, showing a shear-thinning behavior with increasing frequency. Moreover, at the same frequency, the viscosity of the system with the same compositions tended to decline, and this accompanied the increasing the number of FAEs. It is known that HDPE and EVOH are thermodynamically incompatible systems. As the solid EVOH particles are dispersed in the HDPE melt, their surfaces might not be wetted sufficiently. Like the situation where the polymeric melt contacts a rigid repulsive wall,[37] a relative slip might occur at interfaces between the solid platelet and the melt matrix when the specimen deforms at a small amplitude.[38–41] With increasing number of FAEs, the EVOH particles expanded gradually; this gradually brought more interfaces parallel to the direction of the shearing stress, which might have promoted the occurrence of relative slip between phases and resulted in a decline of the complex viscosity of the whole specimen. However, this declining tendency became more distinct when the EVOH content was beyond 20 wt %. It was suggested that after the multistage stretching extrusion process, more platelets might have been formed in the system blended with more EVOH components; this was considered to be beneficial for creating more tortuous paths for diffusing gas molecules.

The effect of the morphological evolution of the specimen through the application of different numbers of FAEs on its $P_{(O2)}$ is shown in Figure 4. For the low-EVOH-filled system (15 and 20 wt % EVOH), there was nearly no distinct change in $P_{(O2)}$ with the application of FAEs. $P_{(O2)}$ was maintained around 2×10^{-14} $cm^3(STP)\cdot cm\ cm^{-2}\cdot s^{-1}\cdot Pa^{-1}$, which was close to that of pure HDPE [5×10^{-14} $cm^3(STP)\cdot cm\ cm^{-2}\cdot s^{-1}\cdot Pa^{-1}$]. When the EVOH contents was increased further beyond 25 wt %, $P_{(O2)}$ of the specimen prepared without FAEs still changed little compared to that of the system filled with 20 wt % EVOH. As one FAE was used, $P_{(O2)}$ decreased more than 10 times and approached 9×10^{-16} $cm^3(STP)\cdot cm\ cm^{-2}\cdot s^{-1}\cdot Pa^{-1}$, which was close to that of pure EVOH [1.7×10^{-16} $cm^3(STP)\cdot cm\ cm^{-2}\cdot s^{-1}\cdot Pa^{-1}$]. However, $P_{(O2)}$ of the blend tended to be stabilized by the application of more FAEs; this suggested that the distribution of the barrier phase had

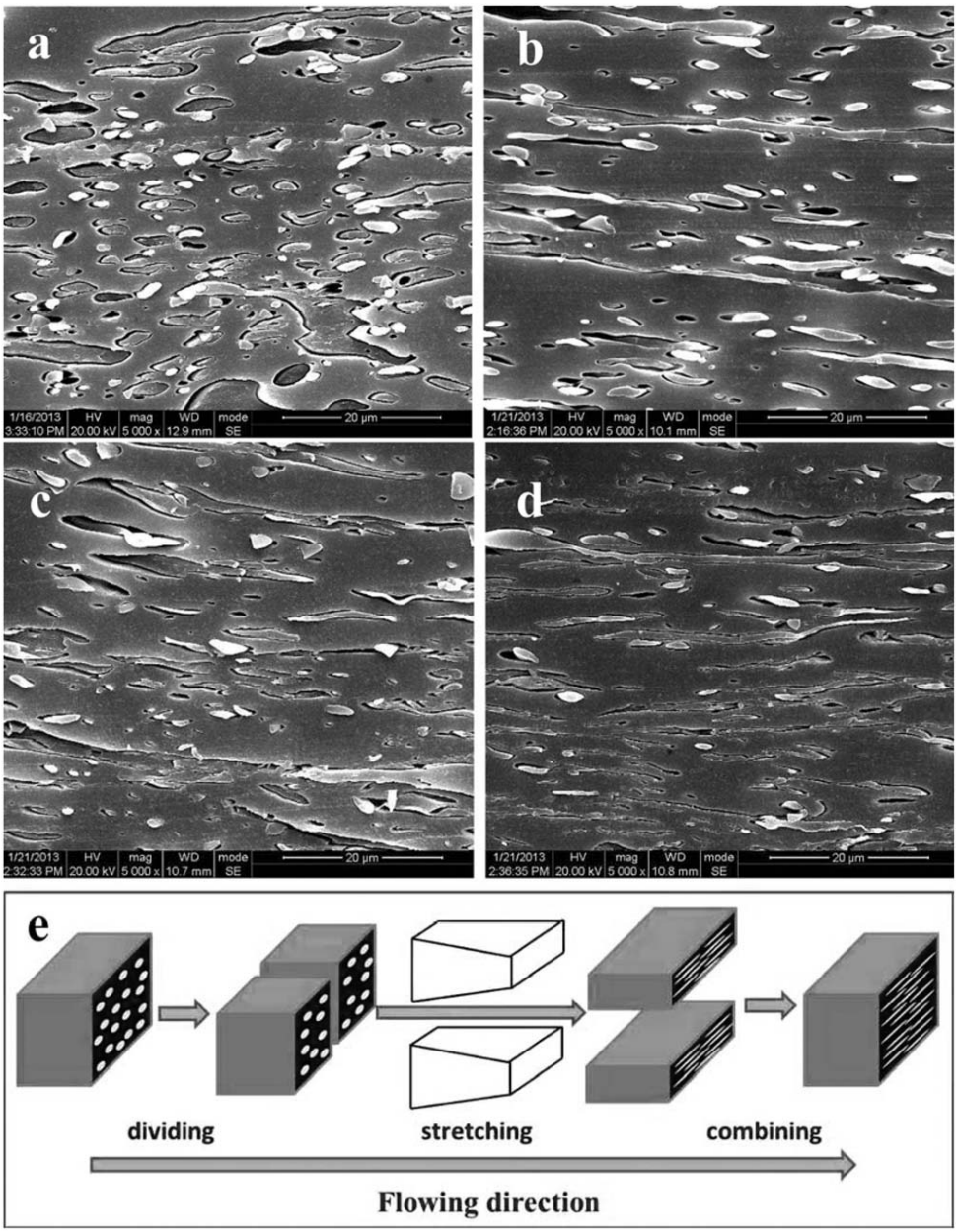

Figure 2. SEM images of the cross sections of the HDPE/EVOH blends (75/25 wt %/wt %) prepared through the application of (a) 0, (b) 1, (c) 2, and (d) 3 FAEs. (e) Schematic of the morphological evolution of the dispersed EVOH phase flowing through one of the FAEs.

created enough tortuosity to hinder the permeation of oxygen molecules. It has to be mentioned that compared with the material prepared through the multistage stretching extrusion, the conventional coextruded films could obtain excellent barrier properties with a lower loading of the barrier phase because of the multilayered structure. Nevertheless, the poor interfacial adhesion between PE and EVOH in coextruded films may hinder their further application. Hence, in our future work, the HDPE/EVOH blend will be coextruded with pure HDPE, which may not only strengthen the interfacial adhesion between layers but may also greatly reduce the EVOH loading when the EVOH is dispersed in the HDPE/EVOH layers as platelets.

In theory, the influence of the geometric morphology of the dispersed barrier phase on the gas permeability can be predicted by the Maxwell model as follows:[42]

$$P = P_c \left[1 + \frac{(1+G)\phi_d}{\left(\frac{(P_d/P_c)+G}{(P_d/P_c)-1}\right) - \phi_d} \right] \quad (1)$$

where P_d and P_c are the permeabilities of the dispersed and continuous phases, respectively; φ_d is the volume fraction of the dispersed phase; and G is a geometric factor that accounts for the shape of the dispersed phase. For a spherelike structure, G is equal to 2. For a cylinder-like structure perpendicular to the

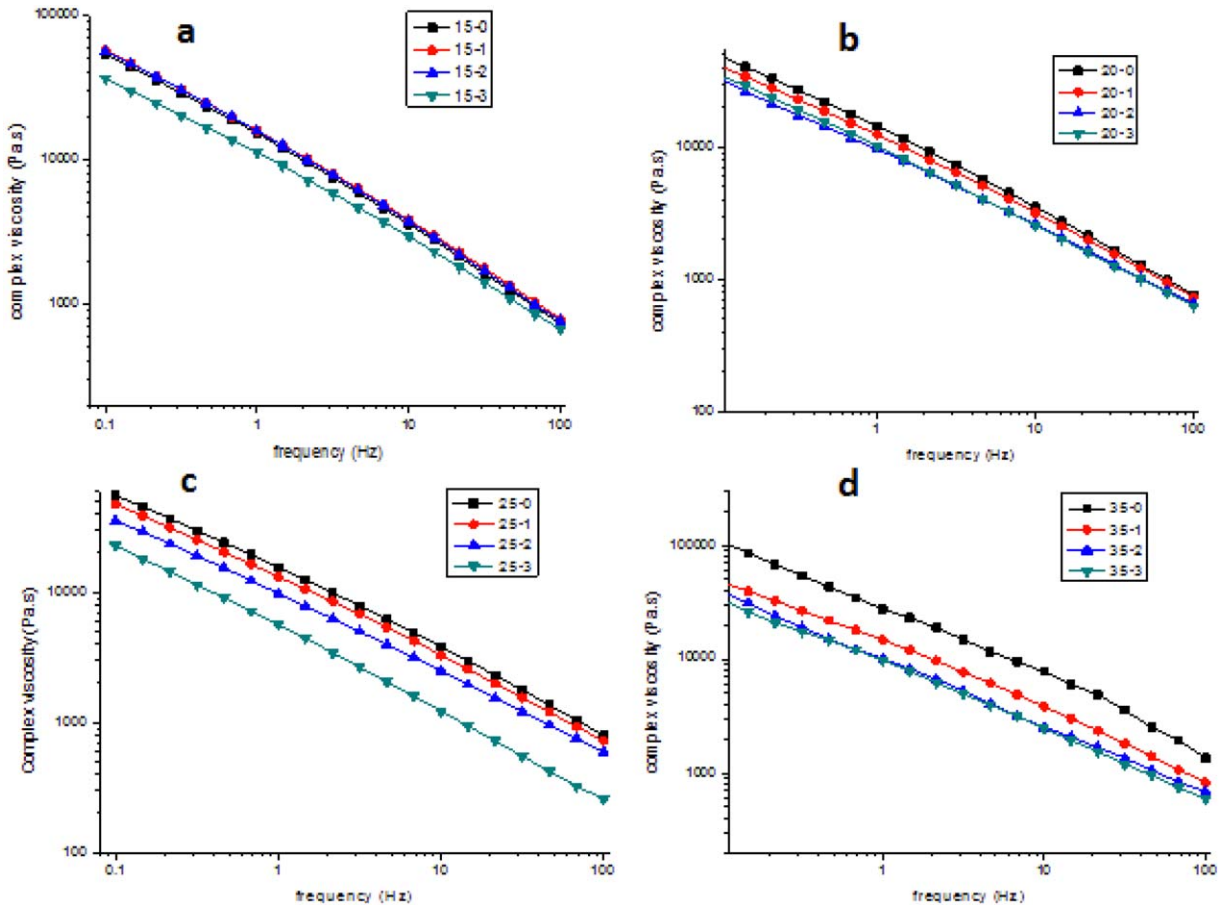

Figure 3. Effect of the number of FAEs on the complex viscosity of the HDPE/EVOH samples blended with (a) 15, (b) 20, (c) 25, and (d) 35 wt % EVOH. [Color figure can be viewed in the online issue, which is available at wileyonlinelibrary.com.]

diffusional flow, G is equal to 1. For a laminate-like structure, G is equal to zero. Hence, the morphological evolution of the dispersed phase experiencing different numbers of FAEs may be described quantitatively through the G value.

Figure 5 compares the G values of the specimens blended with 20 and 25 wt % EVOH due to the different reactions of their $P_{(O2)}$ values to the number of FAEs, as displayed in Figure 4. The calculated results show that for the system blended with 20 wt % EVOH, the G value was basically maintained around 0.2, regardless of the number of FAEs. As the content of EVOH increased to 25 wt %, the G value was distinctly reduced about

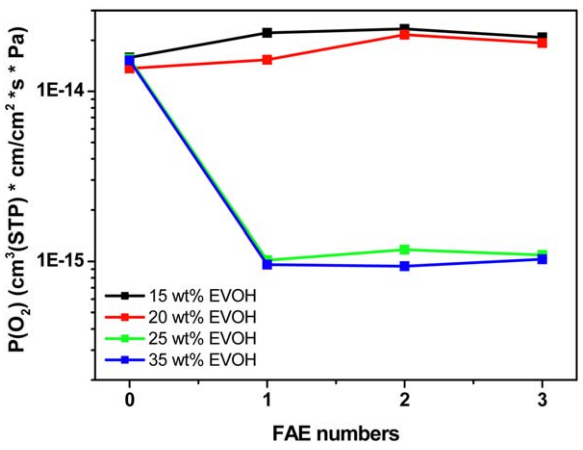

Figure 4. Effect of the number of FAEs on the $P_{(O2)}$ values of the HDPE/EVOH samples blended with 15, 20, 25, and 35 wt % EVOH. [Color figure can be viewed in the online issue, which is available at wileyonlinelibrary.com.]

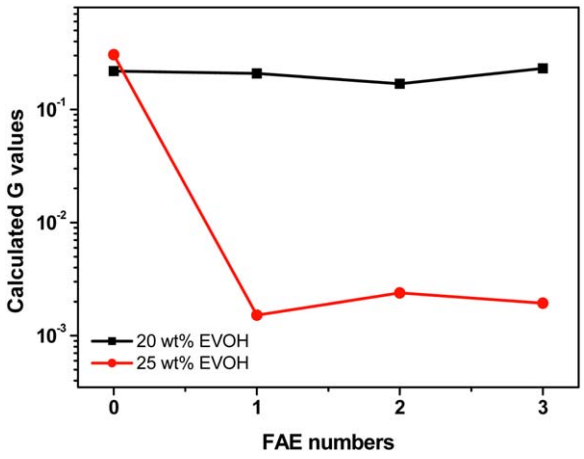

Figure 5. Effect of the number of FAEs on the calculated G values of the HDPE/EVOH samples blended with 20 and 25 wt % EVOH. [Color figure can be viewed in the online issue, which is available at wileyonlinelibrary.com.]

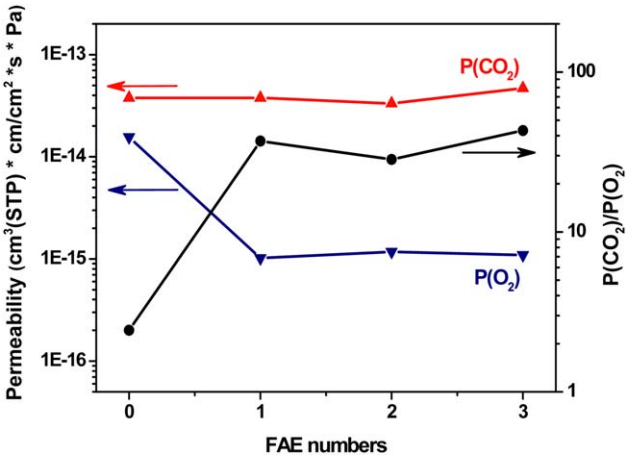

Figure 6. Dependence of the $P_{(O2)}$ values, $P_{(CO2)}$ values, and $P_{(CO2)}/P_{(O2)}$ ratios of the HDPE/EVOH samples blended with 25 wt % EVOH on the number of FAEs. [Color figure can be viewed in the online issue, which is available at wileyonlinelibrary.com.]

two orders of the magnitude compared to the zero-FAE-used system with the application of one FAE. This suggested that the dispersed EVOH phase tended to be expanded into laminate-like morphology after the biaxial-stretching field in the FAEs; this was consistent with the results revealed from SEM images and rheological testing.

The effect of the number of FAEs on $P_{(CO2)}$ of the system blended with 25 wt % EVOH was also investigated. Compared with the $P_{(O2)}$, the applications of FAEs was found to have little effect on $P_{(CO2)}$, as shown in Figure 6; this indicated that $P_{(O2)}$ was especially sensitive to the morphology of the EVOH phase. Actually, other researchers have also reported a similar tendency.[43,44] In contrast to O_2, CO_2 is a kind of acid gas that has a higher permeability to the polar phase because of the humidity existing in the air. Hence, the higher tortuosity in the platelet blend morphology had little influence on $P_{(CO2)}$. As the number of FAEs was increased from zero to three, the calculated $P_{(CO2)}/P_{(O2)}$ ratio tended to be enhanced by about 30 times; this suggested that the platelet formation of EVOH was beneficial for enlarging its selectivity to O_2 and CO_2.

CONCLUSIONS

HDPE/EVOH blends were prepared through multistage stretching extrusion technology that combined an assembly of FAEs with an extruder. With increasing the number of FAEs, the dispersed EVOH phase was transformed into well-defined platelets along the flowing plane because of the biaxial-stretching field existing in each FAE. Compared with the previous biaxial-stretching method, multistage stretching extrusion provides an simple and economic way to generate a laminar structure of the dispersed phase in the matrix phase without the application of an external stretching force. The formation of the platelets was considered to enlarge the interfaces between the dispersed barrier phase and the matrix, causing their relative slip in the shearing process and leading to a decline in the complex viscosity of the whole specimen. However, the expansion of the barrier phase also brought more tortuous paths for the diffusing gas molecules. Compared with that of the non-FAE specimen blended with 25 wt % EVOH, its $P_{(O2)}$ was decreased more than one order of magnitude when one FAE was applied. The structural model for permeability indicated that the enhanced barrier resulted from the increased tortuosity of the diffusion pathway provided by the aligned high-aspect-ratio platelets. On the contrary, these platelets were found to have little effect on $P_{(CO2)}$. This suggested that the material has potential applications in gas separation.

ACKNOWLEDGMENTS

The authors are grateful to the National Natural Science Foundation of China for its financial support of this work (contract grant numbers 51203097, 51227802, and 51073099).

REFERENCES

1. Zhong, Y.; Janes, D.; Zheng, Y.; Hetzer, M.; Kee, D. D. *Polym. Eng. Sci.* **2007**, *47*, 1101.
2. Osman, M. A.; Rupp, J. E.; Suter, U. W. *Polymer* **2005**, *46*, 8202.
3. Yang, L.; Zhang, A.; Wang, L.; Chen, R.; Zeng, Y.; Wu, W. *Polym. Eng. Sci.* **2013**, *53*, 2093.
4. Samios, C. K.; Kalfoglou, N. K. *Polymer* **1998**, *39*, 3863.
5. Wang, Q.; Qi, R.; Shen, Y.; Liu, Q.; Zhou, C. *J. Appl. Polym. Sci.* **2007**, *106*, 3220.
6. Mueller, C. D.; Nazarenko, S.; Ebeling, T.; Schuman, T. L.; Hiltner, A.; Bear, E. *Polym. Eng. Sci.* **1997**, *37*, 355.
7. Ebeling, T.; Norek, S.; Hasan, A.; Hiltner, A.; Bear, E. *J. Appl. Polym. Sci.* **1997**, *71*, 1461.
8. Thellen, C.; Schirmer, S.; Ratto, J. A.; Finnigan, B.; Schmidt, D. *J. Membr. Sci.* **2009**, *340*, 45.
9. Lei, F.; Du, Q.; Li, T.; Li, J.; Guo, S. *Polym. Eng. Sci.* **2013**, *53*, 1996.
10. Wang, H.; Keum, J. K.; Hiltner, A.; Bear, E.; Freeman, B.; Rozanski, A.; Galeski, A. *Science* **2009**, *323*, 757.
11. Wang, H.; Keum, J. K.; Hiltner, A.; Bear, E. *Macromolecules* **2009**, *42*, 7055.
12. Mackey, M.; Flandin, L.; Hiltner, A.; Bear, E. *J. Polym. Sci. Part B: Polym. Phys.* **2011**, *49*, 1750.
13. Dooley, J.; Hyun, K. S.; Hughes, K. R. *Polym. Eng. Sci.* **1998**, *38*, 1060.
14. Anderson, P. D.; Dooley, J.; Meijer, H. E. H. *Appl. Rheol.* **2006**, *16*, 198.
15. Levitt, L.; Macosko, C. W. *J. Rheol.* **1997**, *41*, 671.
16. Schrenk, W. J.; Alfrey, T. *Polym. Eng. Sci.* **1969**, *9*, 393.
17. Osman, M. A.; Atallah, A. *Macromol. Rapid Comm.* **2004**, *25*, 1540.
18. Osman, M. A.; Rupp, J. E.; Suter, U. W. *J. Mater. Chem.* **2005**, *15*, 1298.
19. Subramanian, P. M. *Polym. Eng. Sci.* **1985**, *25*, 483.
20. Faisant, J. B.; Ait-Kadt, A.; Bousmina, M.; Deschenes, L. *Polymer.* **1998**, *39*, 533.

21. Subramanian, P. M.; Mehra, V. *Polym. Eng. Sci.* **1987**, *27*, 663.
22. Lee, S. Y.; Kim, S. C. *Polym. Eng. Sci.* **1997**, *37*, 463.
23. Gopalakrishnan, R.; Schultz, J. M.; Gohil, R. M. *J. Appl. Polym. Sci.* **1995**, *56*, 1749.
24. Kamal, M. R.; Jinnah, I. A.; Utracki, L. A. *Polym. Eng. Sci.* **1984**, *24*, 1337.
25. Favis, B. D.; Chalifoux, J. P. *Polym. Eng. Sci.* **1987**, *27*, 1591.
26. Utracki, L. A.; Shi, Z. H. *Polym. Eng. Sci.* **1992**, *32*, 1824.
27. Wu, S. *Polym. Eng. Sci.* **1987**, *27*, 335.
28. Horák, Z.; Kolařík, J.; Šípek, M.; Hynek, V.; Večerka, F. *J. Appl. Polym. Sci.* **1998**, *69*, 2615.
29. Yeo, J. H.; Lee, C. H.; Park, C. S.; Lee, K. J.; Nam, J. D.; Kim, S. W. *Adv. Polym. Technol.* **2001**, *20*, 191.
30. Kwon, O.; Zumbrunnen, D. A. *Polym. Eng. Sci.* **2003**, *43*, 1443.
31. Shen, J.; Wang, M.; Li, J.; Guo, S.; Xu, S.; Zhang, Y.; Li, T.; Wen, M. *Eur. Polym. J.* **2009**, *45*, 3269.
32. Shen, J.; Li, J.; Guo, S. *Polymer* **2012**, *53*, 2519.
33. Du, Q.; Jiang, G.; Li, J.; Guo, S. *Polym. Eng. Sci.* **2010**, *50*, 1111.
34. Huang, H. J. *Reinf. Plast. Compos.* **2001**, *20*, 356.
35. Jang, J.; Lee, D. K. *Polymer* **2004**, *45*, 1599.
36. Gupta, M.; Lin, Y.; Deans, T.; Baer, E.; Hiltner, A.; Schiraldi, D. A. *Macromolecules* **2010**, *43*, 4230.
37. Aharoni, S. M. *Polym. Adv. Technol.* **1998**, *9*, 169.
38. Zhao, R.; Macosko, C. W. *J. Rheol.* **2002**, *46*, 145.
39. Zhang, J.; Lodge, T. P.; Macosko, C. W. *J. Rheol.* **2006**, *50*, 41.
40. Park, H. E.; Lee, P. C.; Macosko, C. W. *J. Rheol.* **2010**, *54*, 1207.
41. Lee, P. C.; Morse, D. C.; Macosko, C. W. *J. Rheol.* **2009**, *53*, 893.
42. Jarus, D.; Hiltner, A.; Baer, E. *Polymer* **2002**, *43*, 2401.
43. Gontard, N.; Thibault, R.; Cuq, B.; Guilbert, S. *J. Agric. Food Chem.* **1996**, *44*, 1064.
44. Kim, J. H.; Ha, S. Y.; Lee, Y. M. *J. Membr. Sci.* **2001**, *190*, 179.